SLP cluster parameters for predicting ISMR are different in contrasting phases of ESI tendency. During positive (negative) ESI tendency, only SLP (ST) cluster parameters are sufficient to predict ISMR. The skill in ISMR prediction can be improved using different prediction equations depending upon the phase of ESI tendency.

1. Gadgil, S. and Gadgil, S., The Indian monsoon, GDP and agriculture. *Econ. Polit. Wkly*, 2006, **XLI**, 4887–4895.
2. Verma, R. K., Subrmaniam, K. and Dugam, S. S., Interannual and long-term variability of the summer monsoon and its possible link with northern hemispheric surface air temperature. *Proc. Indian Acad. Sci.* (*Earth Planet. Sci.*), 1985, **94**, 187–198.
3. Mooley, D. A. and Paolino Jr, D. A., A predictive monsoon signal in the surface level thermal field over India. *Mon. Weather Rev*., 1988, **111**, 339–352.
4. Gowariker, V., Thapliyal, V., Kulshrestha, S. M., Mandal, G. S., Sen Roy, N. and Sikka, D. R., A power regression model for long range forecast of southwest monsoon rainfall over India. *Mausam*, 1991, **42**, 125–130.
5. Parthasarathy, B., Rupa Kumar, K. and Sontakke, N. A., Surface and upper air temperatures over India in relation to monsoon rainfall. *Theor. Appl. Climatol.*, 1990, **42**, 93–110.
6. Parthasarathy, B., Rupa Kumar, K. and Kothawale, D. R., Surface pressure and summer monsoon rainfall over India. *Adv. Atmos. Sci*., 1992, **9**, 359–366.
7. Krishna Kumar, K., Soman, M. K. and Rupa Kumar, K., Seasonal forecasting of Indian summer monsoon rainfall. *Weather*, 1995, **50**, 449–467.
8. Liu, X. and Yanai, M., Relationship between the Indian monsoon rainfall and the tropospheric temperature over the Eurasian continent. *Q. J. R. Meteorol. Soc*., 2001, **127**, 909–937.
9. Robinson, D. A., Bamzai, A. and Ramsay, B., Evaluating northern hemisphere snow cover during the satellite era: variations in extent and associations with temperature. In Proceedings of the 12th Symposium on Global Change and Climate Variations, American Meteorological Society, Albuquerque, NM, USA, 2001, pp. 36–39.
10. Ye, H. and Bao, Z., Lagged teleconnections between snow depth in northern Eurasia, rainfall in Southeast Asia and sea surface temperatures over the tropical Pacific Ocean. *Int. J. Climatol.*, 2001, **21**, 1607–1621.
11. Zhao, P. and Chen, L. X., Interannual variability of atmospheric heat source/sink over the Qinghai-Xizang (Tibetan) plateau and its relation to circulation. *Adv. Atmos. Sci.*, 2001, **18**, 106–116.
12. Rajeevan, M., Winter surface pressure anomalies over Eurasia and Indian summer monsoon. *Geophys. Res. Lett.*, 2002, **29**, 94-1–94-4.
13. Robock, A., Mu, M., Vinnikov, K. and Robinson, D., Land surface conditions over Eurasia and Indian summer monsoon rainfall. *J. Geophys. Res. D*, 2003, **108**, D4, 4131.
14. Sahai, A. K., Grimm, A. M., Satyan, V. and Pant, G. B., Long-lead prediction of Indian summer monsoon rainfall from global SST evolution. *Climate Dyn.*, 2003, **20**, 855–863.
15. Sahai, A. K., Chattopadhyay, R. and Goswami, B. N., SST based large multi-model ensemble forecasting system for Indian summer monsoon rainfall. *Geophys. Res. Lett.*, 2008, **35**, 1–9.
16. Ertoz, L., Steinbach, M. and Kumar, V., Finding clusters of different sizes, shapes, and densities in noisy, high dimensional data. In Proceedings of Third SIAM International Conference on Data Mining, San Francisco, USA, May 2003.
17. Boriah, S., Simon, G., Naorem, M., Steinbach, M., Kumar, V., Klooster S. and Potter, C., *Predicting Land Temperature Using Ocean Data*, KDD Seattle, WA, USA, 2004.
18. Kakade, S. B. and Kulkarni, A., Relationship between ESI tendency and Indian monsoon rainfall: a possible mechanism. *Atmos. Sci. Lett.*, 2012, **13**, 22–28.
19. Kakade, S. B. and Kulkarni, A., The changing relationship between surface temperatures and Indian monsoon rainfall with the phase of ESI tendency. *Adv. Meteorol.*, 2012, doi: 10.1155/2012/934624
20. Jarvis, R. A. and Patrick, E. A., Clustering using a similarity measure based on shared nearest neighbors. *IEEE Trans. Comput.*, 1973, **C-22**, 1025–1034.
21. Kripalani, R. H. and Kulkarni, A., Climatology and variability of historical Soviet snow depth data: some new perspectives in snow – Indian monsoon teleconnections. *Climate Dyn.*, 1999, **15**, 475–489.

ACKNOWLEDGEMENTS. We thank Prof. B. N. Goswami, Director, Indian Institute of Tropical Meteorology, Pune for providing the necessary facilities. We also thank the anonymous reviewers for providing useful suggestions that helped improve the manuscript.

Received 6 June 2013; revised accepted 30 August 2013

Plant height profiling in western India using LiDAR data

P. Tripathi* and M. D. Behera

Centre for Oceans, Rivers, Atmosphere and Land Sciences,
Indian Institute of Technology, Kharagpur 721 302, India

Plant height has always been a subject of research in forest and vegetation sciences. Space-borne LiDAR data of Geoscience Laser Altimeter System (GLAS) on the Ice, Cloud and land Elevation Satellite (ICESat) have opened up new possibilities to analyse vegetation height. Here, we have analysed the plant height panorama for various forest vegetation classes of western India and understood their profile in terms of topography, vegetation canopy density and presence of heterogeneous features within the LiDAR footprints. Of the total 14,230 LiDAR hits for western India falling in 32 forest vegetation classes, we eliminated extreme plant height ranges to retain 9553 (67.13%) data points for further analysis. Maximum number of data points was observed over temperate coniferous forest, pine forest and desert dune scrub with 2119, 936 and 1770 number of LiDAR hits respectively. The maximum and minimum plant height range varied between 70 and 2.2 m for temperate coniferous forest and alpine scrub. In general, we noticed inaccuracy in the plant height estimates from GLAS data points for higher slope and elevation. Overestimation in data points could be attributed to the presence of anthropogenic features, viz. buildings, settlement and

*For correspondence. (e-mail: tripathy.poonam@gmail.com)

towers; and underestimation could be attributed to bare ground, agricultural field and water body owing to class heterogeneity and positional inaccuracy. This study provides a profile of plant heights from western India that can be used for structural characterization studies utilized in climate and ecological assessments.

Keywords: Forest management, LiDAR data, plant height, remote sensing, vegetation classes.

THE importance of vegetation canopy height has always been a research topic in forest mapping, habitat quality, biodiversity and carbon cycle[1,2]. LiDAR remote sensing can provide three-dimensional vegetation structure[3–5] by accurately capturing the spatial patterns of canopy heights[6] and serves as a surrogate in stand succession state prediction[7] and spatial variation patterning[8]. LiDAR has been proven better compared to optical and microwave-based remote sensing estimates in its ability to predict biomass in temperate deciduous, temperate coniferous forests[9,10].

LiDAR is an active remote sensing technique in which a pulse of laser energy is transmitted towards the surface. The principle of operation of radar and LiDAR is similar in those pulses of energy at wavelengths ranging from millimetres to metres for radar and 0.5–10 μm for LiDAR are transmitted onto the ground. This transmitted pulse of energy further interacts with the medium or objects under study, and scattered back to the instrument. The backscattered light captured by the LiDAR's receiver is used to determine the properties of the medium through which the beam propagated. The pulses are time-tagged and travel with a known velocity in a given medium. Thus, by knowing the time delay created by travel of laser beam from source to the target surface and back to the sensor is measured and provides a distance or range. Hence the common use of the term 'laser altimetry'. The range calculation was given by Vosselman and Mass[11] (eq. (1))

$$\rho = c\tau/2n, \tag{1}$$

where τ is the round-trip time delay of the laser beam, c the velocity of light, and n is the correction factor equal to the reflective index of the atmosphere.

The limitations of passive remote sensing technologies in capturing the horizontal and vertical aspects of forest structure, biomass and misrepresentation of canopy structure, spectral features and bidirectional responses led to emergence of active remote sensing as a potential tool[7,12,13]. The advantage of using LiDAR remote sensing for forestry applications is that it can provide three-dimensional vegetation structure[3–5] by accurately capturing the spatial patterns of canopy heights[6], characterizing vertical distribution of canopy material, crown volume, sub-canopy topography, biomass, vertical foliage diversity and multiple layers, height to live crown, large tree density, leaf area index, and physiographic or life-form diversity through direct and indirect retrievals. It has enormous potential for forest ecological research, because it directly measures the physical attributes of vegetation canopy structure that are highly correlated with the basic plant community measurements[14].

Space-borne LiDAR data of Geoscience Laser Altimeter System (GLAS) on the Ice, Cloud and land Elevation Satellite (ICESat) open the possibility to map global forest vertical structure. ICESat/GLAS acquired the global data of emitted light pulse of known duration and intensity during 2003 to 2009, which was transmitted, absorbed and scattered throughout the vegetation canopy by leaves and branches at various depths[13–17]. Lefsky[12] developed an approach to map forest height globally using GLAS, which showed strong relationship with height prediction. GLAS-derived global vegetation height product produced more realistic dominant vegetation height for tropical forests between 30 and 60 m versus 20 and 40 m (ref. 13).

Studies demonstrated the potential of GLAS data to characterize forest structure; though surface topography still needs special attention on GLAS sensitivity. Many forest locations with steep slopes and high surface roughness contribute to stretched waveforms due to large footprint resulting in mixed vegetation return of LiDAR hits[18,19]. According to empirical studies[20,21], vegetation height estimation in hilly landscape and steep slopes is challenging due to complex terrain. Leeuwen and Nieuwenhuis[22] reviewed the possible causes of overestimation and underestimation of tree height, wherein they proposed the terrain slope as a strong factor. Random digital elevation model (DEM) errors can also cause under- and overestimation of slopes[23]. Variation in terrain elevation or tree height over a small area leads to inaccurate retrieval of tree height. Los *et al.*[13] demonstrated the application and sensitivity analysis of filters based on the tests of slope, elevation, area under first Gaussian, amplitude of first Gaussian, sigma and neighbour. Here, we evaluated the performance of GLAS-retrieved tree height data and compared them with field and literature-based estimates. Pre-processed vegetation height data were acquired from Los *et al.*[13] for utilization in the study (pers. commun.). The basic pre-processing steps to retrieve the vegetation height data from GLAS waveform (GLA14) conversion are mentioned here. The GLA14 data distributed in binary format were converted into ASCII format by the IDL program developed by the National Snow and Ice Data Centre at University of Colorado Cooperative Institute for Research in Environmental Sciences (CIRES), United States. Then, the waveform data, originally in counts from 0 to 255, were converted into voltage units and the voltage waveform was normalized after which waveforms were smoothed by a Gaussian filter. Finally, Gaussian components were fitted to the smoothed waveform. Detailed descriptions of these

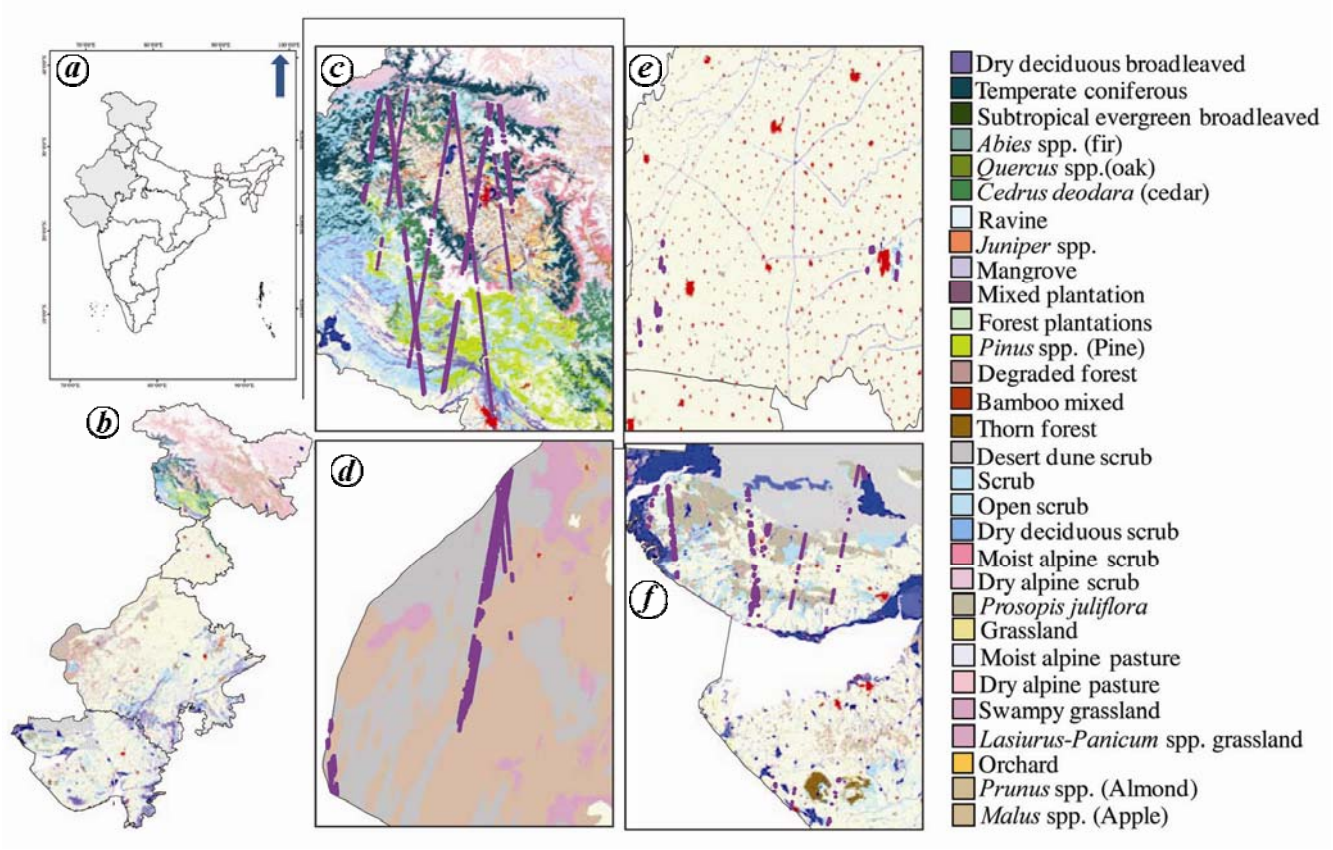

Figure 1. Four states of northwestern India considered for the study (***a***) under the backdrop of the forest vegetation type map[29] (***b***), falling in the upper Himalayan zone (***c***), the great Indian Thar Desert (***d***), agricultural field-dominated zone of Punjab (***e***) and coastal vegetation zone of Gujarat (***f***) wherein LiDAR hits are shown over the forest vegetation and land-use classes.

processing steps are given in Duong *et al.*[24]. Los *et al.*[13] employed the method of Rosette *et al.*[25] (eq. (2)) to retrieve vegetation height as

$$h_V = 1.06(r_1 - r_{A1,2}), \quad (2)$$

where h_V is the vegetation height, r_1 the signal start, and $r_{A1,2}$ is the the centroid range increment for maximum amplitude between Gaussians 1 and 2.

Spurious data were inspected and filtered out using SRTM-derived DEM for land surface topography. Comparison with GLAS-derived elevation was also helpful to obtain indication about slope.

The study area encompasses parts of northwestern India, including states of Jammu & Kashmir (J&K), Punjab, Rajasthan and Gujarat (Figure 1 *a*). The study site is a complex mountainous area in Western Himalaya (J&K) that shares international boundaries with Pakistan and China. Punjab is an intensively cultivated state having >84% area under agriculture, whereas Rajasthan is the largest state of India in terms of geographic area, mostly occupied by Thar, the great Indian desert. Gujarat is situated on the western coast of the country having the longest coastline. The region accommodates several forest vegetation classes ranging from grasslands, thorn forests and mangroves to alpine pastures with an altitudinal variation from minimum 1 m amsl in Rajasthan to 4500 m amsl in J&K, thereby representing a conspicuous site for the study.

ICESat/GLAS acquired data globally during 2003–2009. GLAS, a full waveform sensor uses a 1064 nm laser operated at 40 Hz, emits laser pulses of 7 ns width equivalent to 1 m (1 ns = 15 cm) in surface elevation and records the returned laser energy from an ellipsoidal footprint of approximate diameter of 70 m on ground spaced at 175 m along track on ground surface. The footprints include backscattered energy of different objects on the ground, where the return signal is described as a function of time; this will lead to multiple return echoes. Being a full waveform system, GLA14 data are capable of recording the full return signal and thereby provide information about the vertical structure of the footprint representing a voxel with an elevational value in three-dimensional space with a vertical resolution of less than 3 cm. Waveform extent is the vertical distance between the first and last elevation at which the waveform energy exceeds a threshold level. There are basically two categories of LiDAR systems – discrete return devices (DRD)

Table 1. Tree height ranges collected from the literature and used in the present study

Forest/dominant vegetation class	Tree height (m)	Altitude (m)	Study site	References	Tree height (m) taken in this study
Temperate coniferous	24–88	1373–3600	Indian Himalaya, Malam Jabba in Pakistan	35–37	4–70
Cedrus deodara	11–80	1200–3000	Doda (J&K), Pauri, Garhwal District (Uttarakhand) of Indian Himalaya, Pakistan	35, 37–39	5–70
Abies spp. (fir)	26–75	1373–3050	India, Pakistan	35, 37	4–70
Pinus spp. (pine)	15–42	450–2300	Garhwal Himalaya (Uttarakhand), Solan (Himachal Pradesh), Pakistan	40–43, 37	4–60
Quercus spp. (oak)	2–30	1800–3000	Meghalaya, Pakistan	44–45, 37	6–30
Sub-tropical broad leaved evergreen	25–30	–	India, Columbia	46, 47	Up to 55
Juniper spp.	1–20	–	Western Himalaya	48	Up to 40
Prunus spp. (almond)	15	–	Jammu & Kashmir	49–51	2–15
Malus spp. (apple)	8–10	1860–2900	Himachal Pradesh	52–54	15
Prosopis juliflora scrub	3–14	–	Western India	55, 56	0.3–14
Tropical thorn forest	6–10	–	India, Pakistan	57, 58	0.5–5
Mangrove	5–10	–	India, Pakistan	37, 59	0.5–6
Lasiurus – Panicum grassland	1–2.5	–	Rajasthan	60	5
Saffron	0.1–0.5	–	Jammu & Kashmir	61–63	0.5–2

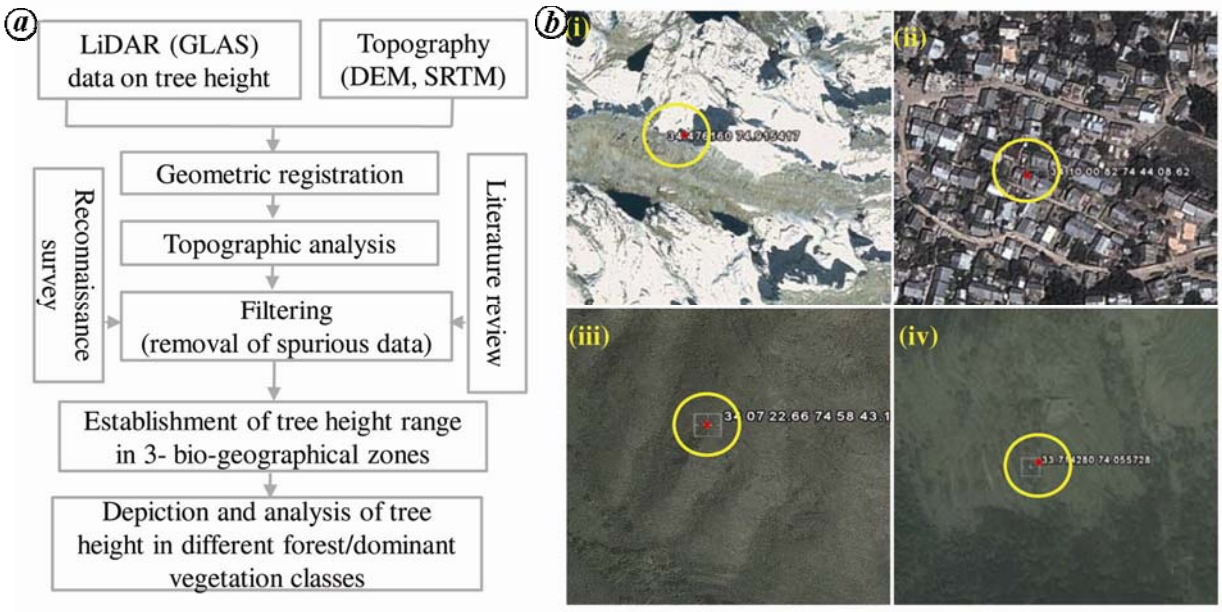

Figure 2. ***a***, Methodology for tree height analysis. ***b***, Snapshots of the locations with misrepresentation of tree height in different vegetation types: (i) Moist alpine pasture, overestimated height 62.4 m at slope 12°, altitude 3291 m. (ii) Forest plantation, overestimated height, 45 m. (iii and iv) Temperate coniferous and pine forest with LiDAR hits on ground due to open canopy. Image Source: *Google Earth*, NOAA, 2007.

and waveform recording devices (WRD). The former measures time elapsed between emission and return of laser pulse, while the later captures continuous energy return from each emitted laser pulse[26] and is more efficient in providing enhanced vertical structure of forests[9]. The pre-processed tree height GLAS land data (GLA14) product, release 31, was gathered for the study[13]. The interpolated shuttle radar topographic mission (SRTM) data (version 4.1) distributed by the Consultative Group for International Agriculture Research Consortium for Spatial Information (CGIAR-CSI) was procured and processed to obtain an indication of the slope for the Indian region[27,28].

The raw (non-filtered) vegetation height LiDAR data and SRTM DEM were geometrically corrected and projected to Universal Transverse Mercator (UTM) reference system using GIS tool. Slope and altitude were extracted using the LiDAR data points for the corresponding locations. Forest vegetation type map prepared during 'Biodiversity characterization at landscape level' project was

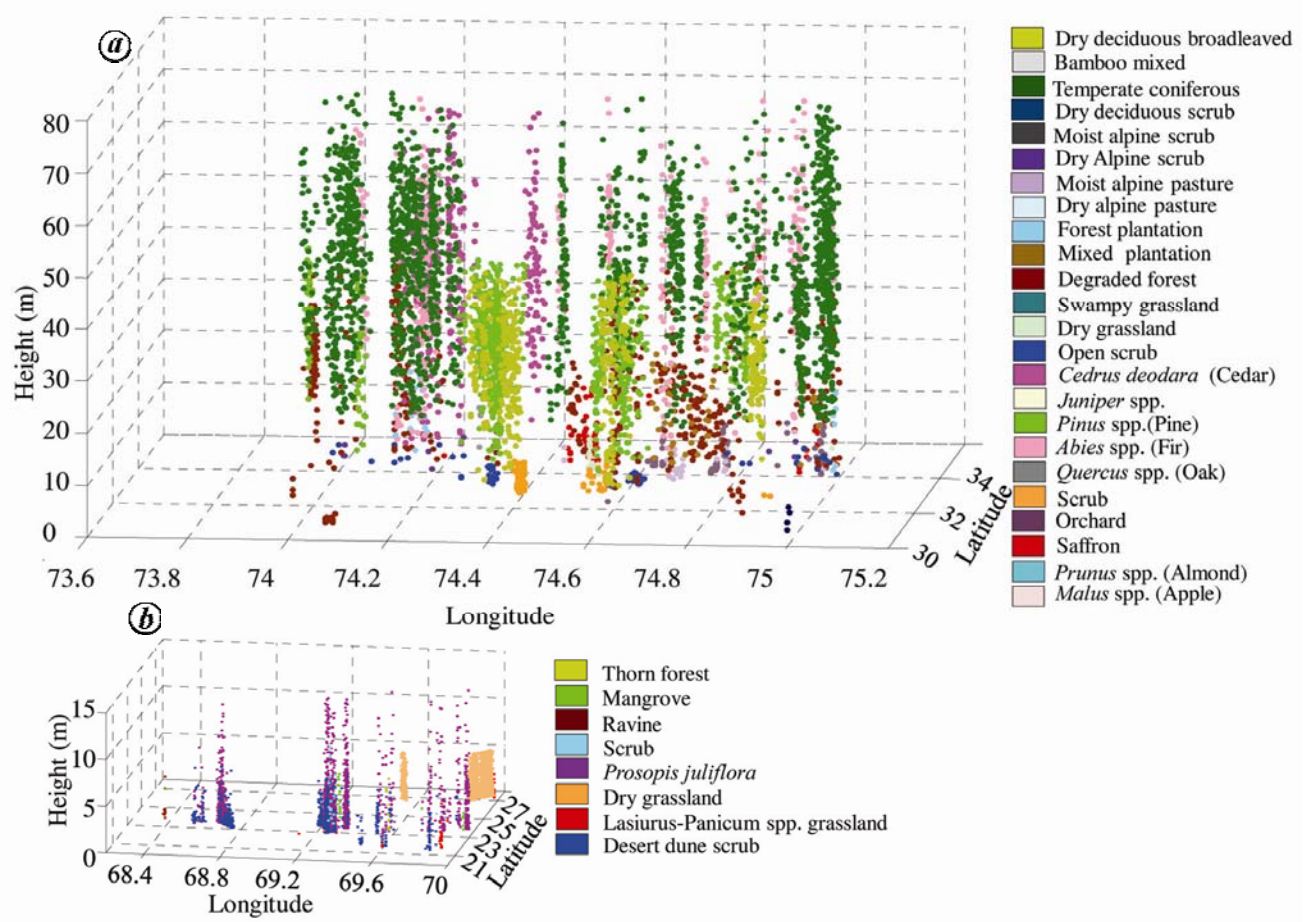

Figure 3. Three-dimensional representation of plant height profile in (***a***) upper Himalayan and (***b***) lower arid and coastal zones according to GLAS land data (GLA14) with filtration.

utilized as reference for the study site[29]. Information gathered during the reconnaissance survey (carried out during 2005) was utilized for forest vegetation characterization. A detailed literature survey helped in compilation of plant height ranges (Table 1), which provided a basis to eliminate/filter values for different forest vegetation classes for further analysis. Explanation in terms of topography, vegetation canopy density and presence of heterogeneous features within the LiDAR footprints was obtained from *Google Earth*, NOAA (2007) and SRTM DEM (Figure 2 *a* and *b*). Further, the plant height data points were converted to a voxel grid using a geometric, three-dimensional representation to analyse the height ranges of different forest vegetation classes and depicted in three parts (Figure 3 *a* and *b*).

Out of 14,230 LiDAR hits for 32 forest vegetation classes, 26 were observed in the upper Himalayan zone, while 6 were observed in the lower arid and coastal zone (Figure 1 *b*). Information on plant height ranges, their altitudinal distribution, site locations and their publication sources is mentioned along with the plant height ranges in Table 1. On elimination/filtration of extreme plant height ranges, 32.87% data points was dropped, permitting 9553 (67.13%) data points for further analysis (Table 2). Maximum number of data points was observed over temperate coniferous, pine and desert dune scrub classes with a total number of 2119, 936 and 1770 LiDAR hits respectively; while minimum number of data points was observed under broadleaved evergreen, orchard and dry deciduous scrub classes (Table 2). Of all vegetation types the minimum plant height observed to be 2.2 m for alpine scrub and maximum 70 m for temperate coniferous forest respectively. This plant height approached up to 15 m for *Prosopis juliflora* scrub in upper Himalayan zone and 5.7 m for mangroves in lower arid and coastal zones respectively (Figure 3 *a* and *b*).

In general, we noticed inaccuracy in the plant height estimates from GLAS data for points of higher slope and elevation (Figure 2 *b*, i). Maximum number of plant height overestimation was found on >10° slope and altitude beyond 2000 m in the subalpine region covered with scrub and pasture vegetation that confirms the observation by Yang *et al.*[19] and Xing *et al.*[21] for >15° slope

Table 2. Percentage of overestimated and underestimated LiDAR hits

Forest/dominant vegetation class	No. of total LiDAR hits	LiDAR hits with under-estimation (%)	LiDAR hits with over-estimation (%)	Possible causes of underestimation	Possible causes of overestimation
Temperate coniferous	2,267	99 (4.37)	49 (2.16)	–	–
Cedrus deodara (Deodar)	389	7 (1.80)	8 (2.06)	–	Slope >10
Abies spp. (fir)	447	9 (2.01)	22 (4.92)	–	–
Pinus spp. (pine)	1,159	13 (1.12)	210 (18.12)	–	Interspersed with other species
Quercus spp. (oak)	21		8 (38.10)	Open forest (ground hit)	–
Tropical broad layered evergreen	1	–	–	Open forest (ground hit)	Slope >10, undulating terrain, ridges
Juniper spp.	208	–	183(87.98)	–	Slope >10, interspersed with other species
Prunus spp. (almond)	97	2 (2.06)	23 (23.71)	Open forest (ground hit)	Slope >10
Bamboo mixed	9	–	5 (55.56)	–	Slope >10, undulating terrain
Dry deciduous forest	554		97 (17.51)	–	Slope >10, undulating terrain
Degraded forest	481	6 (1.35)	131 (27.23)	Open forest (shrub)	Slope >10, undulating terrain
Malus spp. (apple)	5	–	4 (80)	Bare ground	Interspersed with other species and structures
Bamboo mixed	9	–	5 (56)	–	–
Forest plantation	70	15 (21.43)	8 (11.43)	Agriculture, bare ground	Anthropogenic features
Mixed plantation	413	56 (13.56)	97 (23.49)	Bare ground, water body	Slope >10, interspersed with other species and structures
Prosopis juliflora scrub	1,819	156 (8.58)	109 (5.99)	–	–
Orchard	107	3 (2.80)	33 (30.84)	Bare ground	Slope >10
Desert dune scrub	2,231	–	461 (20.66)	–	Slope >10
Dry alpine scrub	128	–	116 (90.63)	–	Slope >10, high altitude, trees, undulating terrain, ridges
Dry deciduous scrub	9	–	6 (66.67)	–	Interspersed with other species, industrial activity
Moist alpine scrub	61	–	57 (93.44)	–	Slope >10, high altitude + trees
Open scrub	2,047	–	1,946 (95.07)	–	Slope >10, high altitude
Scrub	1,240	–	518 (41.77)	–	Undulating terrain
Dry grassland	52	–	10 (19.23)	–	Slope >10, interspersed with other species
Lasiurus–Panicum grassland	23	–	2 (8.70)	–	Slope >10
Swampy grassland	52	–	10 (19.23)	–	Slope >10
Dry alpine pasture	45	–	30 (66.67)	–	Slope < 20, interspersed with other species, sudden undulation
Moist alpine pasture	155	–	125 (80.65)	–	Slope < 20, interspersed with other species, sudden undulation
Saffron	31	–	28 (90.32)	–	Slope >10
Thorn forest	11	–	–	–	–
Mangrove	60	–	–	Bare ground	–
Ravine	29	3 (10.34)	7 (24.14)	Bare ground, water body	Anthropogenic features
Total	14,230	369 (2.59)	4,308 (30)		

Slope is in degrees; (–) indicates not applicable.

conditions. Few data points showed overestimation that could be attributed to the presence of many anthropogenic features, viz. buildings, settlements and towers. Maximum overestimations were observed for open scrub (95.07%), moist alpine (93.44%) and dry alpine scrub (90.63%) classes (Table 2), which spread 11–30° in slope and 2000–4000 m altitude for open scrub, 11–13° slope and 2000–4000 m altitude for moist alpine scrub and 11–21° slope and 2000–4100 m altitude for dry alpine scrub. With reference to *Google Earth*, NOAA (2007) and SRTM DEM, we found that these data points fall on undulating terrain, extreme ridges and sharp valleys that might have contributed to overestimation (Figure 2 *b*, i). Los *et al.*[13] also implemented a slope filter to eliminate erroneous data points for slope >10°. As observed, plant height data points from GLAS waveform can be affected

by slope variations and the waveform from a slope without vegetation may give an impression of vegetation canopy over a flat surface[25,30]. Figure 2 *b* shows the snapshots of four vegetation types from *Google Earth*, depicting the overestimation of tree height for moist alpine pasture and forest plantation and underestimation for temperate coniferous and pine vegetation. Most of the plant height underestimation was observed in temperate coniferous (4.37%), pine (1.12) and plantation (21.43%) as the footprint might have been received from other targets such as bare ground, agricultural field and water body owing to class heterogeneity and positional inaccuracy (Figure 2 *b*, ii–iv). This study provides a profile of plant heights of western India that can be utilized in plant growth models and study of structural characterization. GLAS data provide a sum of Gaussian peaks in return signal and also a single tree height through the waveform extent[31], and have been used for various practical applications such as land cover classification, canopy height modelling, and above-ground biomass estimation[32,33]. Moreover, its global coverage and cost-effectiveness provide a prospective for forest structure modelling. However, slope effect in varied topography results in complications in extracting canopy height from raw waveform due to mixed returns from ground[13,31]. To account for such hitches few slope correction algorithms have already been applied to provide the precise results with better vertical accuracy[23,31,32]. LiDAR technology offers an emerging challenge to the management of India's forests, the panorama of which ranges from evergreen tropical rainforests in the Andaman and Nicobar Islands, the Western Ghats and the northeastern states, to dry alpine scrub high in the Himalaya to the north. The technology could be utilized to address various aspects of forest ecosystem management, not possible previously with the data available from aerial photographs, optical and radar satellites or even by ground measurements. If cautiously planned, LiDAR can form the most scientific and accurate means of forest management in the country, viz. the three-dimensional dataset can be used to redefine the only existing 'forest types' classification[34] that groups Indian forests into 16 major and 22 minor types based on structure, physiognomy and floristic properties of vegetation.

1. Humphrey, J., Hawes, C., Peace, A., Ferris-Kaan, R. and Jukes, M., Relationships between insect diversity and habitat characteristics in plantation forests. *For. Ecol. Manage.*, 1999, **113**, 11–21.
2. Turner, W., Spector, S., Gardiner, N., Fladeland, M., Sterling, E. and Steininger, M., Remote sensing for biodiversity science and conservation. *Trends Ecol. Evol.*, 2003, **18**, 306–314.
3. Wehr, A. and Lohr, U., Airborne laser scanning – an introduction and overview. *ISPRS J. Photogramm. Remote Sensing*, 1999, **54**, 68–82.
4. Harding, D., Lefsky, M., Parker, G. and Blair, J., Laser altimeter canopy height profiles: Methods and validation for closed-canopy, broadleaf forests. *Remote Sensing Environ.*, 2001, **76**, 283–297.
5. Lefsky, M. A., Cohen, W. B., Parker, G. G. and Harding, D. J., Lidar remote sensing for ecosystem studies. *BioScience*, 2002, **52**, 19–30.
6. Drake, J. B. and Weishampel, J. F., Multifractal analysis of canopy height measures in a longleaf savanna. *For. Ecol. Manage.*, 2000, **128**, 121–127.
7. Dubayah, R. and Drake, J., Lidar remote sensing for forestry. *J. For.*, 2000, **98**, 44–46.
8. Parker, G. G., Structure and microclimate of forest canopies. In *Forest Canopies – A Review of Research on a Biological Frontier* (eds Lowman, M. and Nadkarni, N.), Academic Press, San Diego, 1995, pp. 73–106.
9. Drake, J. B., Dubayah, R. O., Knox, R. G., Clark, D. B. and Blair, J. B., Sensitivity of large-footprint LiDAR to canopy structure and biomass in a neotropical rainforest. *Remote Sensing Environ.*, 2002, **81**, 378–392.
10. Hyde, P. *et al.*, Mapping forest structure for wildlife habitat analysis using waveform LiDAR: validation of montane ecosystems. *Remote Sensing Environ.*, 2005, **96**, 427–437.
11. Vosselman, G. and Mass, H. G., *Airborne and Terrestrial Laser Scanning*, Whittles Publishing, 2009.
12. Lefsky, M. A., A global forest canopy height map from the moderate resolution imaging spectroradiometer and the geoscience laser altimeter system. *Geophys. Res. Lett.*, 2010, **37**, 1–5.
13. Los, S. O. *et al.*, Vegetation height products between 60°S and 60°N from ICESat GLAS data. *Geosci. Model Dev. Discuss.*, 2011, **4**, 2327–2363.
14. Behera, M. D. and Roy, P. S., Lidar remote sensing for forestry applications: the Indian context. *Curr. Sci.*, 2002, **83**, 1320–1327.
15. Zwally, H. J. *et al.*, ICESat's laser measurements of polar ice, atmosphere, ocean, and land. *J. Geodyn.*, 2002, **34**, 405–445.
16. Brenner, A. C. *et al.*, Derivation of range and range distributions from laser pulse waveform analysis. Algorithm theoretical basis document version, 4, 2003.
17. Rosette, J. A. B., North, P. R. J., Suarez, J. C. and Los, S. O., Uncertainty within satellite LiDAR estimations of vegetation and topography. *Int. J. Remote Sensing*, 2010, **31**, 1325–1342.
18. Hancock, S., Understanding the measurements of forests with waveform LiDAR. Ph D dissertation, University College, London, UK, 2010.
19. Yang, W., Ni-Meister, W. and Lee, S., Assessment of the impacts of surface topography, off-nadir pointing and vegetation structure on vegetation LiDAR waveforms using an extended geometric optical and radiative transfer model. *Remote Sensing Environ.*, 2011, **115**, 2810–2822.
20. Chen, Q., Retrieving vegetation height of forests and woodlands over mountainous areas in the Pacific coast region using satellite laser altimetry. *Remote Sensing Environ.*, 2010, **114**, 1610–1627.
21. Xing, Y., de Gier, A., Zhang, J. and Wang, L., An improved method for estimating forest canopy height using ICESat-GLAS full waveform data over sloping terrain: a case study in Changbai mountains, China. *Int. J. Appl. Earth Obs.*, 2010, **12**, 385–392.
22. Leeuwen, V. M. and Nieuwenhuis, M., Retrieval of forest structural parameters using LiDAR remote sensing. *Eur. J. Forest Res.*, 2010, **129**, 749–770.
23. Simard, M., Naiara, P., Joshua, B. F. and Alessandro, B., Mapping forest canopy height globally with spaceborne lidar. *J. Geophys. Res.*, 2011, **116** (G4); doi:10.1029/2011JG001708.
24. Duong, H., Pfeifer, N. and Lindenbergh, R., Analysis of repeated ICESat full waveform data: methodology and leaf-on/leaf-off comparison. In Proceedings: Workshop on 3D Remote Sensing in Forestry, University of Natural Resources and Applied Life Sciences, Vienna (BOKU), 2006, pp. 239–248.
25. Rosette, J. A. B., North, P. R. J. and Suarez, J. C., Vegetation height estimates for a mixed temperate forest using satellite laser altimetry. *Int. J. Remote Sensing*, 2008, **29**, 1475–1493.

26. Mallet, C. and Bretar, F., Full-waveform topographic LiDAR: state-of-the-art. *ISPRS J. Photogramm. Remote Sensing*, 2009, **64**, 1–16.
27. Jarvis, A., Reuter, H. I., Nelson, A. and Guevara, A., Hole-filled SRTM for the globe version 4. Available from the CGIAR-CSI SRTM 90 m database, 2008; http://srtm.csi.cgiar.org
28. Rodriguez, E., Morris, C. S., Belz, J. E., Chapin, E. C., Martin, J. M., Daffer, W. and Hensley, An assessment of the SRTM topographic products. Technical Report NASA JPL D-31639, Jet Propulsion Laboratory, Pasadena, California, 2005, pp. 1–143.
29. Roy, P. S. *et al.*, Biodiversity characterization at landscape level national assessment, 2012.
30. North, P. R. J., Rosette, J. A. B., Suárez, J. C. and Los, S. O., A Monte Carlo radiative transfer model of satellite waveform LiDAR. *Int. J. Remote Sensing*, 2010, **31**, 1343–1358.
31. Lefsky, M. A., Keller, M., Pang, Y., De Camargo, P. B. and Hunter, M. O., Revised method for forest canopy height estimation from Geoscience Laser Altimeter System waveforms. *J. Appl. Remote Sensing*, 2007, **1**, 013537–013537.
32. Lefsky, M. A. *et al.*, Estimates of forest canopy height and aboveground biomass using ICESat. *Geophys. Res. Lett.*, 2005, **32**, L22S02.
33. Boudreau, J., Nelson, R. F., Beaudoin, A., Guindon, L. and Kimes, D. S., Regional aboveground forest biomass using airborne and spaceborne LiDAR in Quebec. *Remote Sensing Environ.*, 2008, **112**, 3876–3890.
34. Champion, H. G. and Seth, S. K., *A Revised Survey of the Forest Types of India*, The Manager of Publications, Delhi, 1968.
35. Anon., Package of practices for forestry crops, 2005, A report published by Director, Directorate of Extension Education, Dr YS Parmar University of Horticulture and Forestry, Nauni, Solan (HP).
36. Sher, H. and Al Yemeni, M., Economically and ecologically important plant communities in high altitude coniferous forest of Malam Jabba, Swat, Pakistan. *Saudi J. Biol. Sci.*, 2011, **18**, 53–61.
37. Sheikh, M. I., *Trees of Pakistan*, Winrock International Institute for Agricultural Development. Pictorial Printers, Pakistan, 1993, pp. 1–142.
38. Khanduri, V. P. and Sharma, C. M., Pollen production, microsporangium dehiscence and pollen flow in Himalayan cedar (*Cedrus deodara* Roxb. ex D. Don). *Ann. Bot.*, 2002, **89**, 587–593.
39. Slathia, P. S., Bhagat, G. R., Swaranjeet, S., Kher, S. K. and Narinder, P., Traditional knowledge on utility of *Cedrus deodara* (Roxb.) loud. in Doda district of Jammu province. *Indian J. Traditional Knowledge*, 2007, **6**, 518–520.
40. Gupta, B., Mehta, R. and Mishra, V. K., Fire ecology of ground vegetation in *Pinus roxburghii* Sargent plantations in north-west Himalaya – floristic composition and species diversity. *Caspian J. Environ. Sci.*, 2009, **7**, 71–78.
41. Rana, T. S., Datt, B. and Rao, R. R., Vegetational diversity in Tons Valley, Garhwal Himalaya (Uttaranchal) India with special reference to phytogeographical affinities of the flora. *Taiwania*, 2001, **46**, 217–231.
42. Sharma, C. M., Khanduri, V. P. and Ghildiyal, S. K., Reproductive ecology of male and female strobili and mating system in two different populations of *Pinus roxburghii*. *Sci. World J.*, 2012, 271389, doi: 10.1100/2012/271389.
43. Nizami, S. M., Mirza, S. N., Livesley, S., Arndt, S., Fox, J. C., Khan, I. A. and Mahmood, T., Estimating carbon stocks in subtropical pine (*Pinus roxburghii*) forests of Pakistan. *Pak. J. Agric. Sci.*, 2009, **46**, 4.
44. Khurram, M. *et al.*, Antibacterial potentials of *Quercus baloot*. *J. Med. Plants Res.*, 2012, **6**, 1244–1249.
45. Khan, M. L. and Tripathi, R. S., Seedling survival growth of early and late successional tree species as affected by insect herbivory and pathogen attack in sub-tropical humid forest stands of north-east India. *Acta Oecol.*, 1991, **12**, 569–579.
46. Parthasarathy, N., Selwyn, M. A. and Udayakumar, M., Tropical dry evergreen forests of peninsular India: ecology and conservation significance. *Trop. Conserv. Sci.*, 2010, **1**, 89–110.
47. Folster, H. G., De Las, S. and Khanna, P., A tropical evergreen forest site with perched water table, Megdalena valley Columbia. Biomass and bioelement inventory of primary and secondary vegetation. *Oecol. Plant.*, 1976, **11**, 297–320.
48. Dar, G. H. and Christensen, K. I., Gymnosperms of the Western Himalaya. 1. The genus *Jumperus* (Cupressaceae). *Pak. J. Bot.*, 2003, **35**, 283–311.
49. Anon., Socio-economic profile of Jammu & Kashmir, Report, Directorate of Economics & Statistics, Jammu & Kashmir, 2008.
50. http://kashmiribhatta.in/plants_animals.php.
51. http://trimorizki12.blogspot.in/2012/04/kashmir-valleys-almond-trees-lure.html44−46.
52. Anon., Apple orchard characterization using remote sensing and GIS for Kinnaur, Chamba and Sirmaur districts in Himachal Pradesh. Project report, Space Application Centre, ISRO, 2008.
53. Mehta, N. S. and Bhatt, N., Remote sensing for apple orchard characterization covering parts of Shimla District. *Indian Soc. Geomatics Newsl.*, 2006, **12**.
54. Rana, J. C., Pradheep, K. and Verma, V. D., Naturally occurring wild relatives of temperate fruits in Western Himalayan region of India: an analysis. *Biodivers. Conserv.*, 2007, **16**, 3963–3991.
55. Pasiecznik, N. M. *et al.*, *The Prosopis juliflora – Prosopis pallida Complex: A Monograph*, HDRA, Coventry, 2001.
56. Kaur, R., Gonzales, W. L., Llambi, L. D., Soriano, P. J., Callaway, R. M., Rout, M. E. and Gallaher, T. J., Community impacts of *Prosopis juliflora* invasion: biogeographic and congeneric comparisons. *PloS One*, 2012, **7**, e44966.
57. Nizami, S. M., Estimation of carbon stocks in subtropical managed and unmanaged forests of Pakistan, Ph D thesis, University of Arid Agriculture, Rawalpindi, 2010.
58. Reddy, M. G., *Forest Ecosystem; Forests, People and Livelihoods*. Approach Paper, 2010.
59. FAO, Mangroves of Asia 1980–2005: Country Reports. Forest resources assessment working Paper No. 137, Rome, 2007b; www.fao.org/forestry/site/mangrove/statistics
60. Pandey, K. C., Roy, A. K. and Malaviya, D. R., Forage crops varieties. Directorate of Indian Grassland and Fodder Research Institute, Jhansi, India, 2011.
61. Nehvi, F. A., Alam, A. and Yasmin, S., Saffron farming in India: The Kashmir Connection, Report, 2010, vol. 42, pp. 9–15.
62. http://www.flowersofindia.net/catalog/slides/Saffron%20Flower.html
63. Madan, C. L., Kapur, B. M., Gupta, U. S., Saffron. *Econ. Bot.*, 1966, **20**, 377–385.

ACKNOWLEDGEMENTS. We thank Dr Sietse Los, Department of Geography, Swansea University, UK for making available the GLAS data over the Indian region. We also thank Dr P. S. Roy, Project Director, National 'Biodiversity characterization at landscape level' project, jointly conducted by the Department of Space and the Department of Biotechnology, Government of India for providing the vegetation map.

Received 16 December 2012; revised accepted 8 July 2013